Numerical modelling of large scale steel fibre reinforced-reinforced concrete beams failing in shear

Ali Amin, Stephen J. Foster

University of New South Wales, Sydney, Australia.

Abstract

Experimental and numerical studies on Steel Fibre Reinforced Concrete (SFRC) over the last 5 decades, or so, have indicated that the post cracking strength of concrete can be improved by providing suitably arranged, closely spaced, wire reinforcement. While the database of experimental and numerical shear tests of SFRC members is extensive, the pool of test data and numerical models, alike, of SFRC beams containing conventional transverse shear reinforcement (stirrups) are limited. The behaviour of full scale steel fibre reinforced-reinforced concrete (SFR-RC) beams are analysed herein using a smeared crack model provided by ATENA 2D integrated with a constitutive law derived after an inverse analysis from prism bending tests. The numerical model is validated against experimental results obtained from four large scale SFR-RC beams and is shown to reasonably model the experimental responses. The model allows a better understanding of SFR-RC structures failing in shear and can be used as a basis for developing new design procedures for such structures.

Keywords

Steel fibres, concrete, shear, stirrups, ATENA.

1 Introduction

Experimental and numerical investigations have shown that the inclusion of steel fibres in concrete, when adopted in adequate quantities, can improve the shear resistance of beams by increasing the post cracking strength of the concrete. Fibres embedded within concrete delay the propagation and growth of cracks by improving the effectiveness of the crack-arresting mechanisms present when beams are subjected to high shear stresses.

Many studies have considered the possibility of utilizing SFRC by assigning a proportion of the shear resisting capacity of beams to the fibres. This has been realized by ACI-318 (2008), and more recently by the *fib* Model Code 2010 (2012) and the Draft Australian Bridge Code: Concrete (2014). Some inconsistencies in some of these approaches, however, have been identified (Foster, 2010; Amin & Foster, 2014).

To accurately model the inherent nonlinear properties of elements composed of SFRC, it is necessary to make use of advanced software which can correctly model concrete fracture. This is of particular importance when crack propagation at the elemental level can significantly influence the global, or structural, response of the member (Foster & Voo, 2004, Foster et al., 2006, Minelli & Vecchio, 2006). To this end, a numerical investigation is undertaken to study, in detail, the development of shear resistant mechanisms in steel fibre reinforced-reinforced concrete beams with and without conventional shear reinforcement using a commercially available Finite Element package, ATENA 2D, developed by Cervenka Consulting (Cervenka et al., 2002).

The numerical model is validated against experimental results obtained from four 5 metre long by 0.3 metre wide by 0.7 metre high rectangular simply supported beams with varying transverse and fibre reinforcement ratios. An evaluation of the transverse stirrup contribution versus fibre contribution to the shear capacity is compiled and recommendations are made for the explicit inclusion of the distinct capacities to existing design models.

2 Experimental Investigation

An experimental program was conducted to investigate the combined effect of steel fibres and traditional transverse reinforcement on the response of large scale beams subjected to four-point loading. Four beams with various fibre and transverse reinforcement ratios were constructed and tested to failure. As the investigation was designed for the specimens to fail in shear, the beams were designed to ensure that flexural tensile failure did not occur.

The specimen dimensions and testing arrangements are shown in Figure 1. The specimens are designated using the notation BX-Y-Z where ‘X’ is the dosage of fibres (in kg/m^3), ‘Y’ is the diameter of stirrup (in mm), and ‘Z’ is the stirrup spacing (in mm) within the critical shear regions. For example, specimen B25-10-450 represents a beam reinforced with 25kg/m^3 of steel fibres and 10mm stirrups spaced at 450 mm c/c.

The longitudinal reinforcement was fabricated from nominally 500 MPa grade, hot rolled, deformed bars. The beams contained two layers of three normal ductility 28 mm diameter tensile reinforcement (N28), which corresponds to a flexural reinforcement ratio of 1.98%.

Two 20 mm diameter longitudinal reinforcing bars (N20) were located at the top section of the beam. The measured yield strength of the longitudinal bars was 540 MPa.

The 2-leg stirrups were fabricated from hard-drawn wire reinforcement and were spaced at 450 mm centres. The 10 mm diameter stirrups had a yield strength of 450 MPa; the 6 mm stirrups had a yield strength of 550 MPa. The steel fibres used in this study were the double end-hooked Dramix® 5D-65/60-BG fibre. The fibres were 0.9 mm in diameter and 60 mm long.

The specimens were cast using a single batch of concrete obtained from a local ready mix supplier. The concrete had a prescribed characteristic compressive strength of 32 MPa and the aggregate used was basalt with a maximum particle size of 10 mm.

All beam specimens were tested in an Instron 5000 kN stiff testing frame and tested under a ram displacement control of 0.3mm/min. A linear strain conversion transducer (LSCT) was placed at the beam mid-span to measure displacement (Figure 1). The reader is referred to Amin and Foster (2014) for further details on the experimental study.

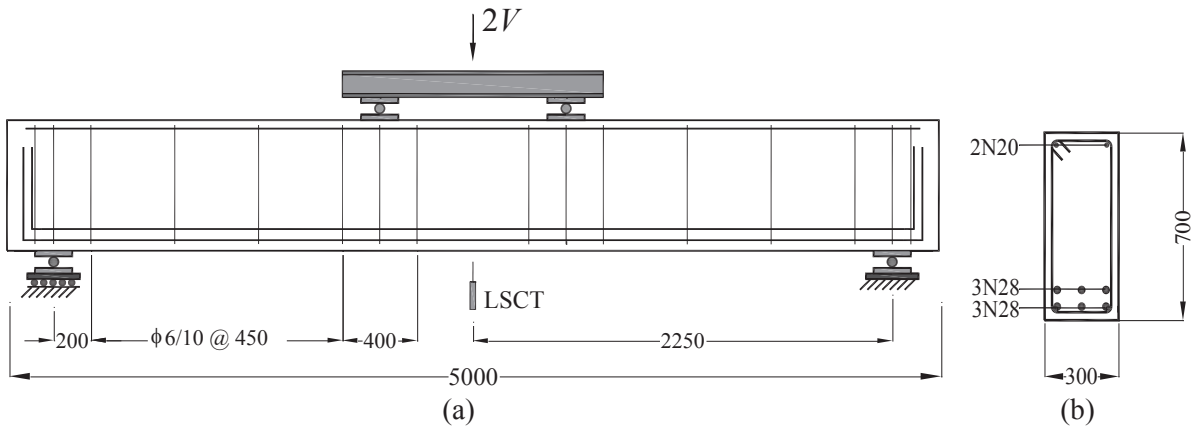

Figure 1: Specimen dimensions (in mm): (a) Test setup; (b) Cross section

3 Mechanical Properties of SFRC

The measured mechanical properties of the SFRC at the time of testing are presented in Table 1. The fracture properties of SFRC were determined directly by obtaining the tensile strength of the concrete matrix, f_{ct}, and the residual tensile strength, $f_{1.5}$ (taken at a crack width of 1.5mm), from six uniaxial 'dogbone' specimens tested to DR AS5100.5 (2014). The tensile properties were also determined indirectly from the residual flexural strength, $f_{R,j}$, through five three-point notched prisms tested to EN 14651 (2007). The mean compressive strength (f_{cm}) and Young's modulus (E_c) were determined by testing three 150 mm diameter x 300 mm cylinders.

Table 1: Mechanical properties of SFRC

f_{cm} (MPa)	E_c (GPa)	f_{ct} (MPa)	$f_{1.5}$(MPa)	f_{R1} (MPa)	f_{R2} (MPa)	f_{R3} (MPa)	f_{R4} (MPa)
34	28	2.45	0.68	2.39	2.52	2.56	2.26

To define the tensile stress versus crack opening displacement fracture constitutive relationship for SFRC, the simplified inverse analysis procedure developed by Amin et al. (2013) was used in this study. The formulation of this model is founded upon a sectional analysis of a prism in bending and considers the influence of fibres on the moment carried by the specimen from the point in the test where the un-cracked concrete has little influence on the prism capacity and considers rigid body rotations. The nominal stress carried by the fibres, $f(w)$, is taken as:

$$f(w) = k_b\left(\frac{f_{R2}}{3} + (f_{R4} - f_{R2})\xi(w)\right) \geq 0 \quad (1a)$$

$$\xi(w) = \frac{w}{3} \times \frac{(D - 0.3h_{sp})}{0.7h_{sp}} - \frac{1}{4} \quad (1b)$$

where D is the total depth of the prism and h_{sp} is the depth less the notch depth. For prisms tested to EN 14651 (2007), $\xi(w)$ (w in mm) simplifies to:

$$\xi(w) = 0.43w - 0.25 \quad (2)$$

The model of Equation 1 is presented generically in Figure 2(a) and corresponding to the experimental data of this study in Figure 2(b). The orientation factors k_t and k_b are applied to the direct tension and prism bending data, respectively, to convert the results to that of an equivalent 3D fibre distribution free of influence of the boundaries (Amin et al., 2013) and taken as:

$$k_t = 0.5 \leq \frac{1}{0.94 + 0.6l_f/b} \leq 1 \quad (3a)$$

$$k_b = \frac{\pi}{3.1 + 0.6l_f/b} \leq 1 \quad (3b)$$

where l_f is the length of the fibre and b is the width of the cross section of the material test.

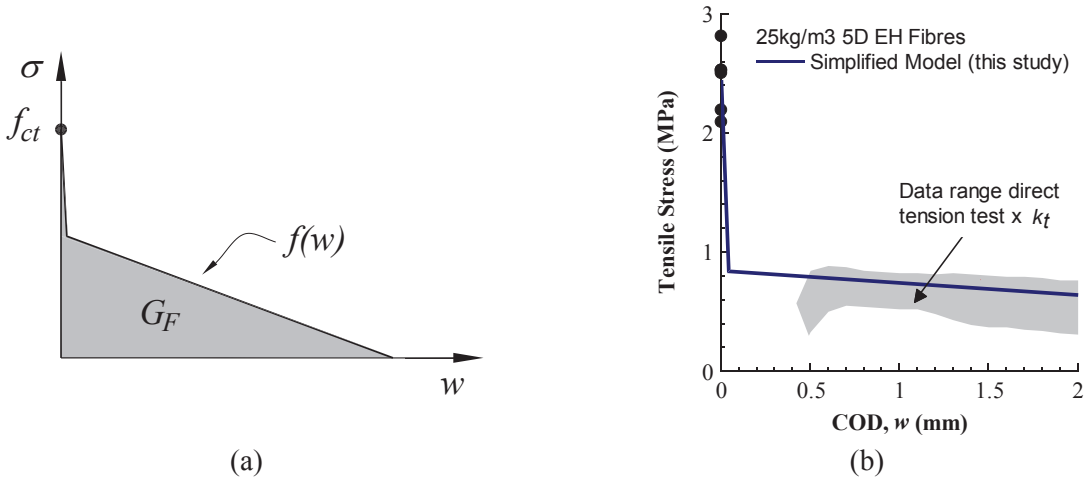

Figure 2: Tensile constitutive law of SFRC: (a) Generic response; (b) Application of inverse analysis procedure of Equation 1 to test data.

4 Finite Element Model

A set of numerical analyses were performed on the four beams of this study utilizing the software ATENA (Cervenka et al., 2002). The material models CC3DNonLinCementitious2 (User) are used in this study to model the concrete and are based on a fracture-plasticity approach which combines constitutive models for tensile (fracture) and compressive (plastic) behaviour.

The fracture model is based on the classical orthotropic smeared crack formulation and crack band model. It utilizes the Rankine failure criterion and is not restricted to any particular shape of hardening or softening laws. A fixed crack approach is used in this study; although there is some debate on whether a rotated crack approach (Minelli & Vecchio, 2006), or combination of both (Foster, 2006) is more appropriate. The plasticity model is founded on the Menetrey-Willam failure surface (Menetrey and Willam, 1995) using a return mapping algorithm for the integration of the constitutive equations. To combine the fracture and plasticity models, a strain decomposition approach introduced by de Borst (1986) is used; that is:

$$\varepsilon = \varepsilon^e + \varepsilon^p + \varepsilon^f \tag{4}$$

where ε^e, ε^p, and ε^f are the elastic, plastic and fracturing strains, respectively. The new stress state in the plastic model is computed using a predictor-corrector formulation where the plastic corrector is computed directly from the yield function of the return mapping algorithm. The crack opening, w, is computed from the summation of the fracturing strain and incremental fracturing strain multiplied by the characteristic length. The full derivation of the material model can be found in Cervenka and Papanikolaou (2008).

For SFRC in compression, no size effects were considered and the concrete is modelled using the nonlinear stress-stain relations given by ATENA; that is:

$$\sigma_c(\varepsilon) = \frac{f_{cm}\left(E_c/E_o - \varepsilon/\varepsilon_c\right)\varepsilon}{\varepsilon_c + \left(E_c/E_o - 2\right)\varepsilon} \tag{5}$$

where E_c, E_o and ε_c are defined in Figure 3(a). This choice reflects the fact that the addition of steel fibres to concrete in conventional dosages, as is in this study, does not have significant influence on the pre-peak compressive properties of the concrete; the post-peak response, however, has been shown to be influenced by the fibre dosage (Mansur et al., 1999). In this study, the post-peak softening curve bears little influence on the numerical study as no phenomena relating to concrete crushing are being studied.

For SFRC in tension prior to cracking the stress-strain relation of SFRC can be described as linear elastic with Elastic Modulus, E_c. A crack is then initiated when the tensile stress exceeds the cracking strength of the matrix, f_{ct} (Rankine criterion). To take account of the residual tensile stresses due to shrinkage, the in-situ tensile strength of the concrete, f_{ct}, is taken as $0.3\sqrt{f_{cm}} = 1.75\text{MPa}$.

The most critical parameter when considering the design of a structural member manufactured with SFRC is its post cracking, or residual, tensile strength. In this paper the constitutive law describing SFRC in tension (Equation 1) is implemented into the ATENA model. A basic assumption of smeared crack models is that the components of the softening stress-strain relationship are uncoupled in the local coordinate system associated with a crack. Taking this assumption into account, the tensile softening behaviour is expressed in terms of stress versus crack opening displacement (σ-w) relationship (Figure 3b). With the material properties given in Table 1 substituted into Equation 1, the tensile relationship for the concrete, f_t, is given as:

$$f_t = \begin{cases} E_c\varepsilon & \text{pre cracking} \\ 1.75 - 22.4w & \text{post cracking, } w < 0.04\text{mm} \\ 0.85 - 0.11w & \text{post cracking, } w \geq 0.04\text{mm} \end{cases} \tag{6}$$

The model allows for an implicit coupling of the components by using a cracking shear modulus that is a function of the Mode I cracking strain; therefore shear transfer across cracks is possible.

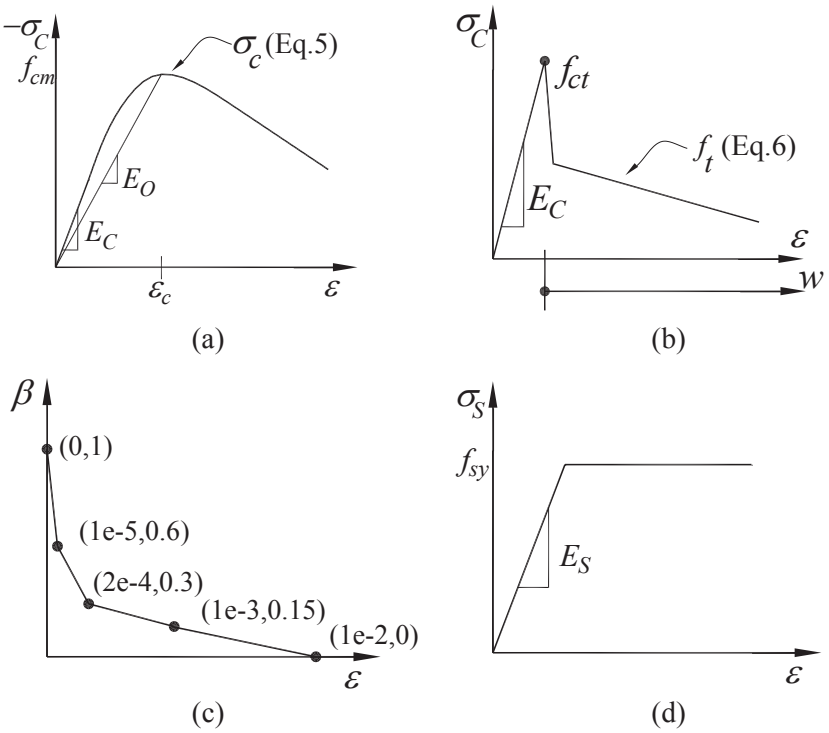

Figure 3: (a) Stress-strain response of SFRC in compression; (b) Response of SFRC in tension; (c) Shear retention factor used in this study; (d) Stress-strain relationship of reinforcing steel

For fixed cracks, the crack system may not be parallel to the principal strain system and shear stresses can evolve along the crack edges. Walraven (1980) showed a dependence between the shear stiffness and the crack width which is taken into account by shear reduction factors. Shear retention functions, $\beta(\varepsilon)$, are sometimes assumed to be constant. The advantage of such a model is that it conserves the independence of the shear and the normal stresses in the cracking zone. However, it is physically not realistic since the shear resistance along a crack is produced by friction, aggregate interlock and fibre bridging; all of which are a function of the crack opening. Moreover, it would imply that even those cracks which have opened up completely (no further stress transfer in tension) would still transmit shear. A more realistic choice is to reduce the materials shear resistance linearly or exponentially with increased crack opening. An exponentially decreasing shear resistance factor is given in Equation 7, where $\bar{\varepsilon}$ is the Mode I strain in the coordinate system associated with the crack, and ε_u is the ultimate strain at which the crack becomes stress free.

$$\beta(\varepsilon) = \left(1 - \frac{\bar{\varepsilon}}{\varepsilon_u}\right)^{\gamma} \tag{7}$$

Larger values of γ correspond to a more pronounced decrease of β in order to simulate higher in-plane shear stress degradation with increased crack opening. In this study we adopt the linearized version of Equation 7 as shown in Figure 3(c).

All reinforcing steels were modelled as simple elastic perfectly plastic materials with perfect bond to the concrete (refer to Figure 3(d)).

To simulate the beams, a 2D model was developed. One half of the beam was modelled with symmetry. The mesh sensitivity of results of the FEA has been checked. For this purpose, the beam was analysed using two different FE meshes (quadrilateral elements limited to 50mm and 100mm). The difference between results of the analyses was negligible. The FE representation of the beams including the mesh and boundary conditions is illustrated in Figure 4. For the notional 50 mm mesh, the model was discretized using 1012 4-node isoparametric membrane elements integrated on a 2x2 quadrature. The non-linear model was solved the using Newton-Raphson method with convergence determined using displacements, out of balance forces and energy and with a solution tolerance of 0.01 for each.

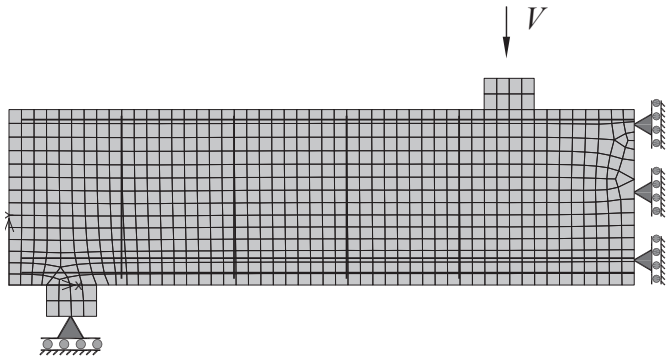

Figure 4: FE representation of shear critical specimens

5 Comparisons with Test Data

The results of the FE modelling are compared with the experimental data in Figure 5 for applied shear versus mid-span deflection. The peak strengths obtained from the FE model are compared to the experimental values and predictions from the alternative model for shear in SFRC in the *fib* Model Code (model appearing on the left hand side of the code) along with the model of the Draft Australian Bridge Code (DR AS5100.5, 2014) in Table 2. In general, the FE model captured the behaviour of the beams well. The model accurately predicts the first cracking load, it models the post cracking stiffness well and the failure loads are reasonably predicted.

In Table 2, two results are presented for the code analyses. In the left column, V_{us} is taken as $nA_{sv}f_{sy,f}$ where n is the number of stirrups that were actually crossed by the shear crack, as observed in the experiment, A_{sv} is the area of the shear reinforcement for one stirrup and $f_{sy,f}$ is the measured mean strength of the transverse reinforcement. In the right column, the values are those predicted by the codes (theory) with the stirrups taken as smeared along the section, as is usual practice. The FEA compares reasonably with predictions from the codes when the actual number of stirrups crossed is considered; the lower result for specimen B25-6-450 is reflective of the fact that in the FEA the failure crack crossed just one stirrup, not two as observed in the tests. In the code analyses with smeared shear steel, the strength may be overestimated. This is because of the significant sensitivity, in the case of large ligature spacing, in the steel contribution if one, two or three stirrups are crossed. For $\theta \approx 34^{o}$ for the SFRC beams, as is the case here, theory suggests that 1.8 ligatures will cross the crack.

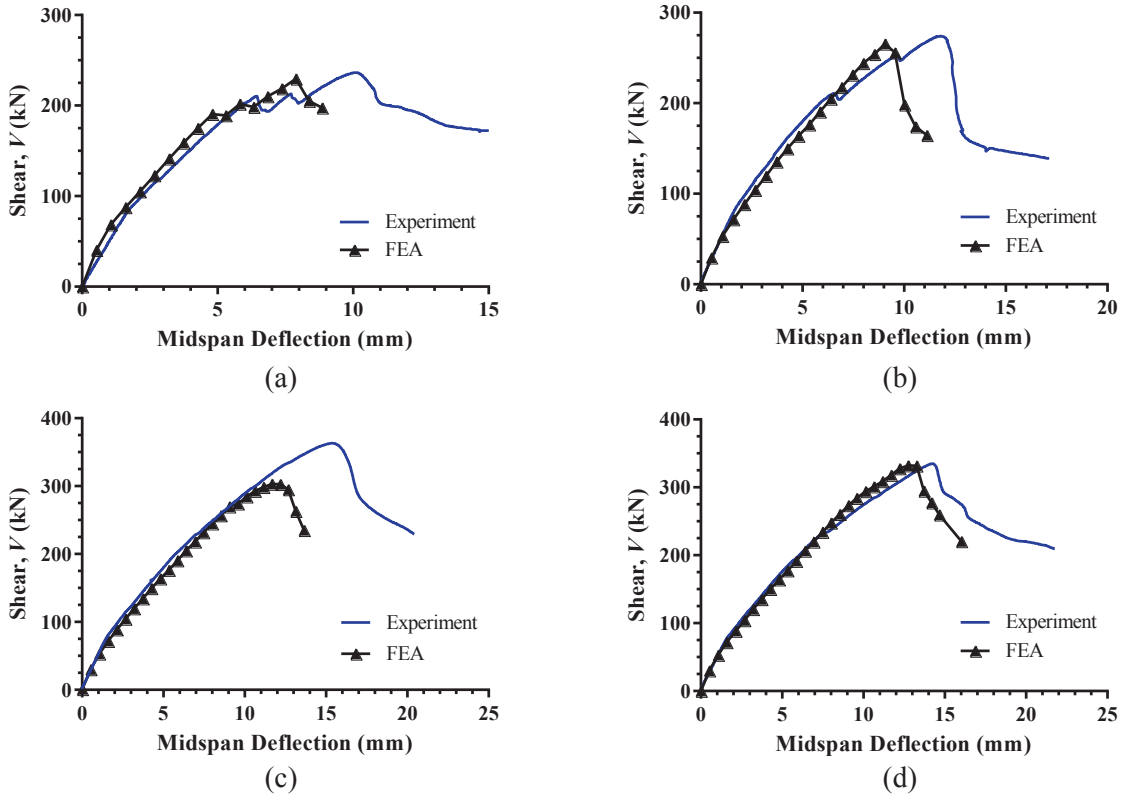

Figure 5: Comparison of FE results against experimental data for beams: (a) B0-10-450; (b) B25-0-0; (c) B25-6-450; (d) B25-10-450

Table 2: Comparison of FE results with experiment and codes

Specimen ID	n	$V_{u,FEA}$ (kN)	$V_{u,exp}$ (kN)	$V_{u,fib}$ (kN)		$V_{u,AS5100.5}$ (kN)	
				With n	Theory	With n	Theory
B0-10-450	1	230	236	235	260	198	274
B25-0-0	0	266	274	249	249	240	240
B25-6-450	2	303	363	300	298	303	308
B25-10-450	1	332	334	307	353	312	388

Figure 6 examines the development of strain and crack formation in beam B25-10-450. At a mid-span deflection of 7 mm (Figure 6a), which corresponds to an applied shear of approximately 210 kN, cracking in the shear span is noticeable. At peak load, (Figure 6b) flexural shear cracks are dominant. The critical crack appears in the model after peak load (Figure 6c) and its location and inclination is comparable to the actual dominant crack observed in the experiment (Figure 6d).

As a fixed crack model is used, the direction of cracking is determined upon the first crack initiation and its orientation is kept fixed afterwards. This is of particular interest in interpreting the results of beam B25-6-450. In the experiment, it was observed that the dominant crack had engaged two stirrups, as opposed to just one in beams B25-10-450 and B0-10-450. In the FEA, the dominant crack passed over just one stirrup in beam B25-6-450 (not two). Adopting the approach of the alternative model for shear in SFRC in the *fib* Model

Code, the prediction of the shear strength of beam B25-6-450 for a failure crack engaging one stirrup is 321 kN and compares well to the FEA result.

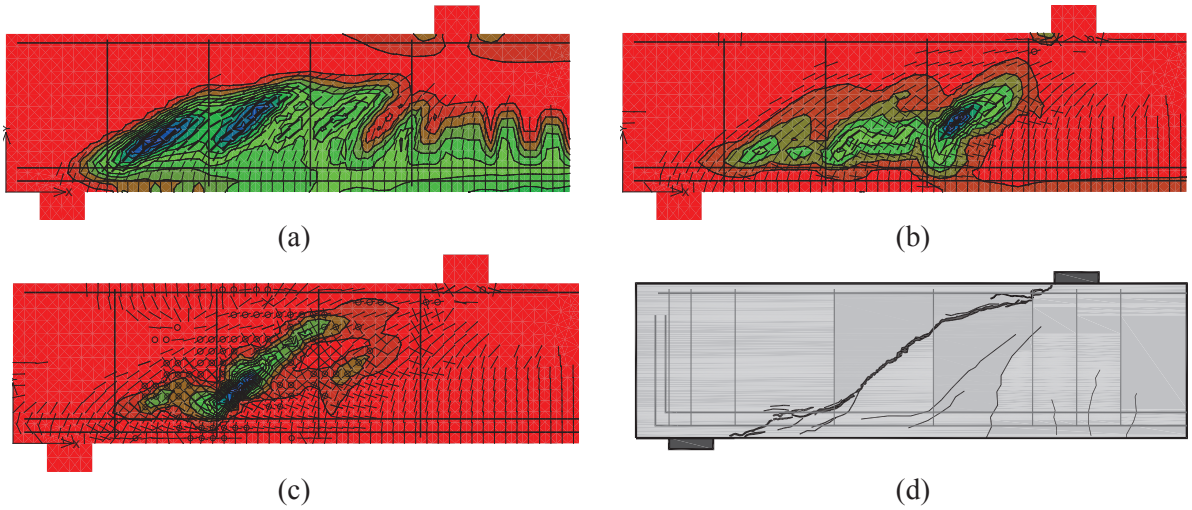

Figure 6: Nonlinear response and crack patterns of beam B25-10-450: (a) Maximum principal strain at 7mm; (b) Maximum principal strain at peak load; (c) Maximum principal strain at 15mm; (d) Actual crack pattern of beam at failure. Figure plotted for 50mm mesh.

6 Conclusions

In this paper a validation of the behaviour of large scale steel fibre reinforced-reinforced concrete beams is made through a comparison of numerical analyses and shear experiments. The numerical analysis was performed using a commercially available software package, ATENA, which was adapted to SFRC using constitutive laws derived from an inverse analysis of prism bending tests. The results of the numerical analysis indicate that the behaviour of SFRC beams can be modelled using ATENA when an appropriate constitutive law in tension is used. The model was shown to compare well with the experimental data in capturing the linear and non-linear responses of the beams.

7 References

ACI 318-11 2008, *Building Code Requirements for Structural Concrete and Commentary*, ACI Committee 318, 456pp.

Amin, A.; Foster, S.J.; and Muttoni, A. (2013), *Evaluation of the Tensile Strength of SFRC as Derived from Inverse Analysis of Notched Bending Tests*. Proceedings of the 8th International Conference on Fracture mechanics of concrete and concrete structures (FraMCoS-8), Toledo, Spain, pp. 1049-1057.

Amin, A.; and Foster, S.J. (2014), *The Behaviour of Steel Fibre Reinforced-Reinforced Concrete Beams in Shear*. Proceedings of the 10th ***fib*** International PhD Symposium in Civil Engineering, Quebec, Canada.

Cervenka, V.; Cervenka, J.; and Pukl, R. (2002), *ATENA – A tool for engineering analysis of fracture in concrete*. Sadhana Academy Proceedings in Engineering Sciences, Vol 27, No 4, pp. 485-492.

Cervenka, J.; and Papanikolaou, V.K. (2009), *Three dimensional combined fracture-plastic material model for concrete*. International journal of plasticity, Vol 24, pp. 2192-2220.

de Borst, R. (1986), *Non-linear analysis of frictional materials*. PhD thesis, Delft University of Technology, Netherlands.

DR AS5100.5 (2014), *Bridge Design Part 5: Concrete*. Draft for Public Comment Australian Standard, Standards Association of Australia.

EN 14651:2007. *Test Method for Metallic Fibre Concrete- Measuring the Flexural Tensile Strength (Limit of Proportionality, Residual)*. European Committee for Standardization, 17pp.

fib Bulletin 66 (2012), *Model code for concrete structures*. fédération internationale du béton (***fib***), Lausanne, Switzerland.

Foster, S.J. (2006), *Limited rotation CMM model for FE analysis of RC membranes*. Progress in Mechanics of Structures and Materials, 19th Australasian Conference on the Mechanics of Structures and Materials, 2006, Christchurch, New Zealand, pp. 177-183.

Foster, S.J.; and Voo, J.Y.L. (2004), *Finite Element Modelling of Fibre Reinforced Concrete Structures*, Developments in Mechanics of Structures and Materials, 18th Australasian Conference on the Mechanics of Structures and Materials, Perth, Western Australia, Eds A. Deeks and H. Hoa, Taylor and Francis, London, pp. 781-787.

Foster, S.J.; Voo, Y.L.; and Chong, K.T. (2006), "Analysis of Steel Fiber Reinforced Concrete Beams Failing in Shear: Variable Engagement Model", Chapter 5 in *Finite Element Analysis of Reinforced Concrete Structures*. Eds. Lowes, L., and Filippou, F., ACI SP-237, 2006.

Foster, S.J. (2010), *Design of FRC beams for Shear using the VEM and the Draft Model Code Approach*. ***fib*** Bulletin No. 57, pp.195-210.

Mansur, M.A.; Chin, M.S.; and Wee, T.H. (1999), *Stress-strain relationship of high-strength fiber concrete in compression*. Journal of Materials in Civil Engineering, ASCE, Vol 11, No 1, pp. 21-29.

Menetrey, P.; and Willam, K.J. (1995), *Triaxial failure criterion for concrete and its generalization*. ACI Structural Journal, Vol 92, No 3, pp. 311-318.

Minelli, F.; and Vecchio, F.J. (2006), *Compression field modelling of fibre reinforced concrete members under shear loading*. ACI Structural Journal, Vol 103, No 2, pp. 244-252.

Walraven, J.C. (1980), *Aggregate Interlock: A theoretical and experimental analysis*. PhD thesis, Delft University of Technology, Netherlands.